ADVANCED MATERIALS

# Supporting Information

for *Adv. Mater.*, DOI: 10.1002/adma.201104535

# Tuning the Properties of ZnO, Hematite, and Ag Nanoparticles by Adjusting the Surface Charge

*Jianhui Zhang,* Guanjun Dong, Aaron Thurber , Yayi Hou,* Min Gu , Dmitri A. Tenne, C. B. Hanna , and Alex Punnoose**

Submitted to ADVANCED MATERIALS

DOI: 10.1002/adma.201104535

# Supporting Information

# Tuning the properties of ZnO, hematite, and Ag nanoparticles by adjusting the surface charge

*By Jianhui Zhang*, Guanjun Dong, Aaron Thurber, Yayi Hou, Min Gu, Dmitri A. Tenne, C. B. Hanna, and Alex Punnoose*

[*] Prof. J. Zhang, Prof. M. Gu
National Laboratory of Solid State Microstructures, Department of Physics,
Nanjing University, Nanjing 210093 (China)
E-mail: zhangjh@nju.edu.cn
G. Dong, Prof. Y. Hou
Laboratory of Immunology and reproductive Biology Medical School, Nanjing University,
Nanjing 210093 (China)
E-mail: yayihou@nju.edu.cn
A. Thurber, Prof. D. A. Tenne, Prof. C. B. Hanna, Prof. A. Punnoose
Department of Physics, Boise State University,
Boise, ID 83725 (USA)
E-mail: apunnoos@boisestate.edu

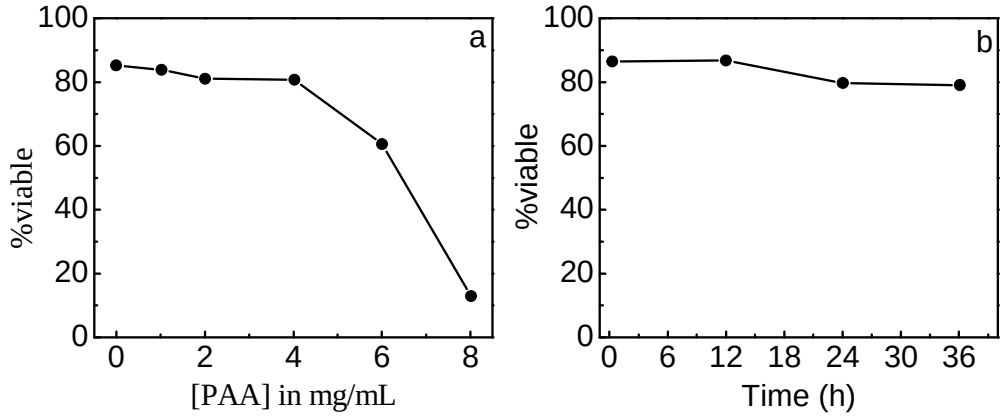


**Figure S1.** Toxicity of PAA with different concentration to Namalwa (a) after 24h treatment, and the time effects on the cytotoxicity of 2mg/mL PAA (b). The PAA cytotoxicity was assessed in the same way as for NPs.

As shown in Figure S1a, PAA has negligible toxicity to Namalwa below 4mg/mL, and its toxicity becomes apparent and enhances with increasing the concentration over 4mg/mL. With the fixed concentration of 2mg/mL, PAA shows negligible toxicity to Namalwa even when the treating time is prolonged to 36h.

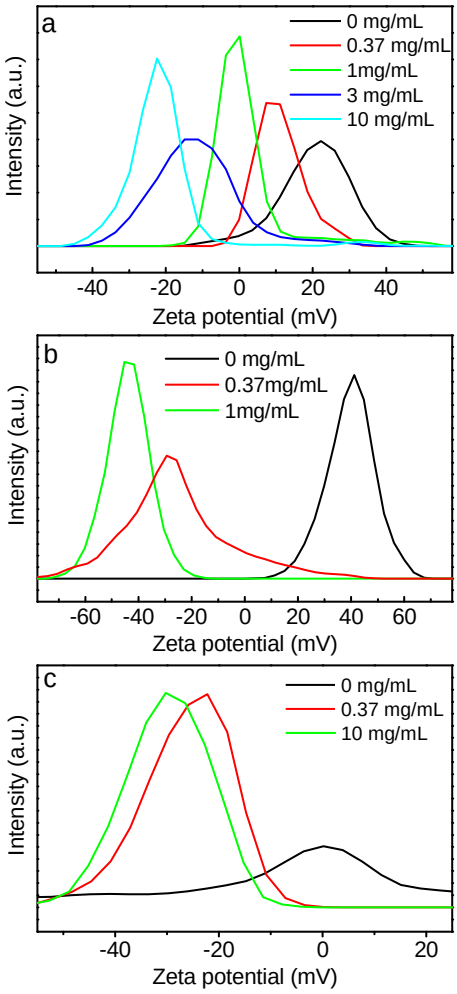


**Figure S2.** Average distribution of ZP intensity for ZnO (a), hetmatite (b), and Ag (c) NPs treated by the aqueous PAA solution with different concentration. With increasing the PAA concentration, the ZP intensity peaks vary in shape and gradually shift to low ZP value, showing that the NP SC is systematically tuned by PAA.

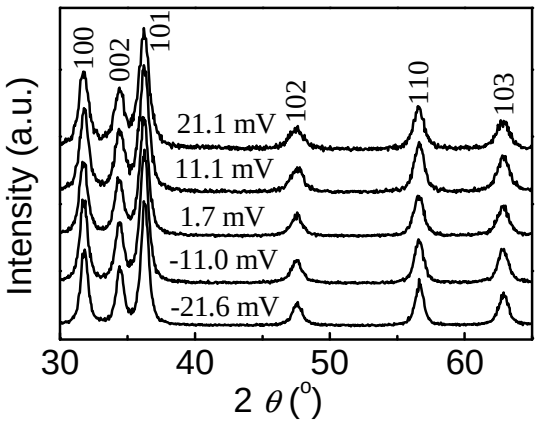


**Figure S3.** XRD patterns of ZnO samples with different SC.

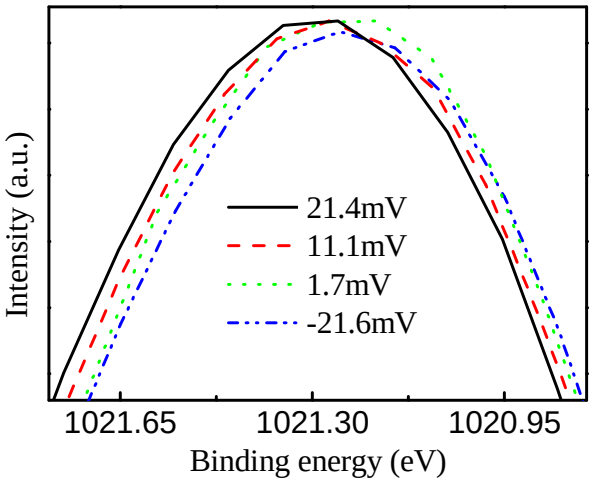


**Figure S4**. Zn $2p_{3/2}$ XPS spectra of selected ZnO samples with different SC. The binding energy scales have been charge referenced using the C1s peak at 284.8 eV.

As shown in Figure S4, upon reducing the ZP (from 21.4 to -21.6mV) by coating with PAA, the Zn $2p_{3/2}$ peak gradually and slightly shifts from 1021.30 to 1021.24 eV. The shift is related to the reduction of Zn valence, which can be attributed to $Zn^{2+}$ ions in ZnO NPs receiving electrons from the coated PAA via the donation of O lone pair electrons. It should be noted that the Zn valence variation induced by the coated PAA is very small, and its influence on the ZnO band gap is undetectable here.

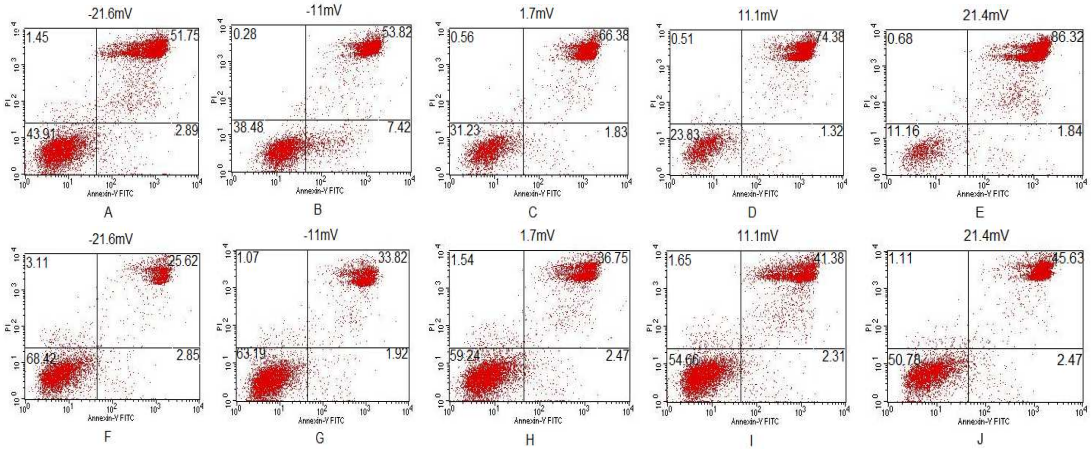


**Figure S5.** Typical quadrant statistics for cytotoxicity assays of ZnO NPs with different SC after 24 h treatment. A-E) the toxicity of ZnO NPs (2mM) to Namalwa cells, F-J) the toxicity of ZnO NPs (1mM) to Raji cells.

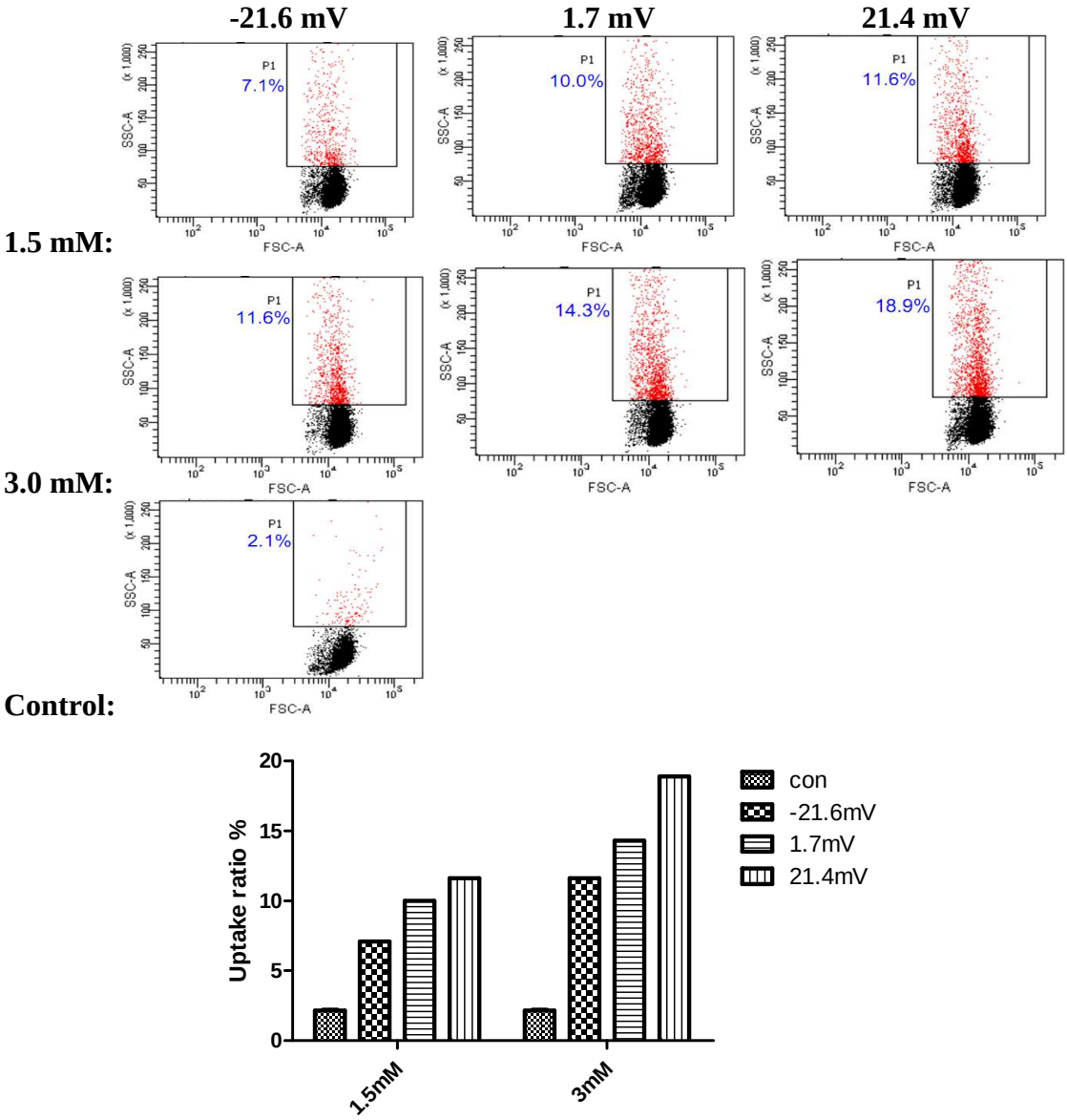


**Figure S6** Uptake of ZnO NPs with different SC and concentration as well as corresponding control without NPs in Raji cells after 2h of treating.

Cellular uptake of ZnO-NPs in Raji cells was examined by flow cytometry. The approach is based on analysis of forward scatter (FSC) versus side scatter (SSC) of measured samples. The SSC value in control cells was subtracted to calculate the SSC distribution ratio in the particle-treated cells for the cellular uptake assay. Cells were incubated with 1.5, and 3.0 mM of ZnO NPs for 2 h, and then washed three times with PBS. After centrifugation, cells were re-suspended in 200ul PBS for flow cytometry. Following gating, control and particle-exposed cells were run and plotted to examine the increase in SSC.

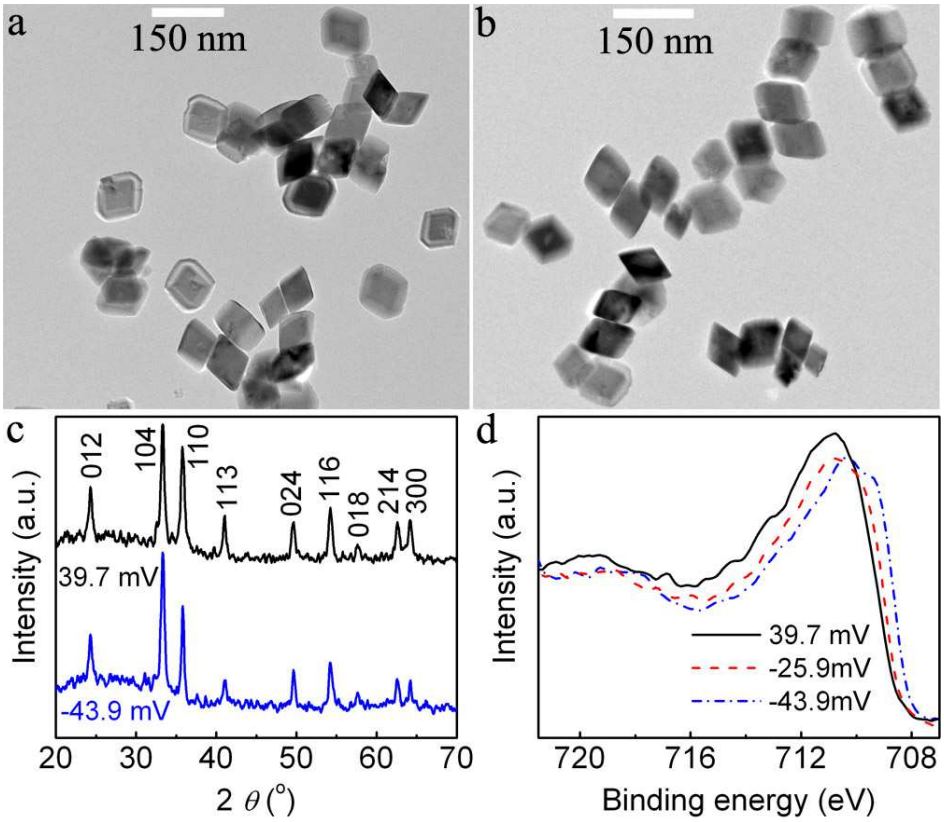


**Figure S7.** Typical TEM images (a: ZP 39.7mV, b: ZP -43.9mV), XRD patterns (c), and Fe $2p_{3/2}$ XPS spectra (d) of the hematite samples with different SC. The binding energy scales in (d) have been charge referenced to the C1s peak at 284.8 eV.

As shown in Figure S7a-c, the XRD patterns and TEM images show that all of the hematite samples have the same pure hexagonal phase ($a$ = 0.504 nm, $c$ = 1.374 nm) and constant average size and cube shape as well as solution dispersion behavior. In other words, the SC variations induced by coating PAA has no detectable influence on the crystal structure, particle size, shape, or dispersion of the hematite nanocubes.

As seen in Figure S7d, the Fe $2p_{3/2}$ XPS peak of the pure hematite samples (ZP 39.7mV) without the coated PAA is located around 710.9 eV, with a satellite peak around 719.5 eV, clearly showing the highly pure hematite phase.[1-2] Reducing the ZP (from 39.7 to -43.9mV) by coating PAA, the Fe $2p_{3/2}$ peak gradually shifts from 710.9 to 710.1 eV. The shift is related to the reduction of Fe valence, which can be attributed to the inference that the $Fe^{3+}$ ions in

hematite NPs receive electrons from the coated PAA via the donation of O lone pair electrons to $Fe^{3+}$. Here it is noted that the binding energy shift induced by the PAA coating in the hematite samples is far larger than that in the ZnO samples. This can be ascribed to the higher oxidative ability of $Fe^{3+}$ ions in comparison to $Zn^{2+}$ ions.

[1] R. S. Cutting, V. S. Coker, J. W. Fellowes, J. R. Lloyd, D. J. Vaughan, *Geochimica et Cosmochimica Acta* **2009**, *73*, 4004.

[2] T. Fujii, F. M. F. de Groot, G. A. Sawatzky, F. C. Voogt, T. Hibma, K. Okada, *Phys. Rev. B* **1999**, *59*, 3195.